Comparative Analysis of Different Synchronous Reluctance Motor Topologies

Claudiu Oprea, Arkadiusz Dziechciarz, Claudia Martis
Department of Electrical Machines and Drives
Technical University of Cluj-Napoca
Cluj-Napoca, Romania
Claudiu.Oprea@emd.utcluj.ro

***Abstract*— Synchronous reluctance machines become more popular nowadays. Development of power electronics allowed reluctance motors to be used in many drive applications. Due to increased interest in electric vehicles and high prices of PMs, the research on electric drives is mainly focused on reluctance machines. Lack of rotor winding lowers copper losses, simplifies power supply system and increases machine's robustness. SynRM produces torque due to rotor's magnetic anisotropy, which is achieved in machines with transversally laminated rotor by introducing flux barriers. The main goal when designing rotor's flux barriers is to achieve the highest saliency ratio possible. However, since operation of the machine depends on interaction between stator magnetic field and the rotor, both stator and rotor's topologies should be taken into account when designing the machine. This paper presents a comparison of SynRMs with stators of three different slot numbers and two different rotor's topologies.**

Keywords—Synchronous Reluctance Machine, Permanent Magnet-free, Electric Vehicles, Finite Element Analysis

I. INTRODUCTION

In the frame of ever increasing concerns on environmental and fossil fuel natural reserves the beginning of the 21st century was marked by the decision of all important car manufacturers to invest in the research and development of electric traction systems. Major developments were reported for the energy storage devices and power electronics components, while the research of electrical machines was focused on high energy density permanent magnet structures. The most widely used types of electric motors for full Electric Vehicles (EV) or (Plug-in) Hybrid Electric Vehicles (P-HEV) are the Interior Permanent Magnet (IPM) and Induction Machine (IM) because of their specific advantages: high torque density (IPM), simple construction and control (IM) [1].

The increase of rare-earth permanent magnet prices caused a shift towards a new generation of permanent magnet-free electric drive systems with high efficiency, high power density, good Noise-Vibration-Harshness (NVH) behavior and safe operation in all conditions: [2]: Switched Reluctance Machine (SRM), DC Excited Flux-Switching Machine (DCEFSM) or Synchronous Reluctance Motor (SynRM) which have all been the topic of research in recent years. While the SRM exhibits high torque ripple and noise and the DCEFSM has all excitation sources on the stator, leading to higher iron losses, the SynRM shows great potential due to its simple construction. The stator of the machine is similar to the one used in conventional IM or Synchronous Machines (SM) and the rotor is obtained from punched laminations. Since the rotor of the synchronous reluctance machine requires no cage or field winding, the machine might be less expensive and more robust than a conventional synchronous machine or cage induction motor. Moreover, lack of field winding in the rotor eliminates the need of sliding contacts, limits iron and copper losses of the machine and allows high speeds.

SynRM, also referred to as Variable Reluctance Synchronous Machine (VRSM), has received little attention in studies on the most appropriate propulsion system for EV, but some authors have shown that it has almost all the advantages of a SRM but with a simplified control and power drive and with better NVH behavior [3,4]. Numerous comparative studies on the performances of the IM and SynRM have been published [5-7], showing that the torque/volume ratio of the latter is similar or superior, while the efficiency is higher because of the smaller losses in the rotor. The main drawback seems to be the lower power factor compared to the one of the IM, with big influence on the efficiency at system level.

The SynRM operating principle was developed more than a century ago [8] and it is based on the reluctance concept for developing torque, requiring that the direct and quadrature axis inductance ratio and difference to be as high as possible. Several rotor structures have been proposed: flux-barrier rotor, segmented rotor (Transversally Laminated Anisotropy - TLA) and Axially Laminated (ALA), as presented in Fig. 1. Initial research was focused on the later topology, using grained oriented magnetic material interleaved by aluminum sheets, but latter studies showed that similar saliency ratios can be obtained with the TLA at reduced manufacturing costs. Another advantage of machine with transversally laminated rotor is that the rotor can be easily skewed, thus allowing the reduction of torque ripple.

The current paper presents a comparative study on the influence of stator topology and rotor geometry on the performances of the SynRM, with focus on the variation of magnetic flux density distribution in the air gap, variation of direct and quadrature inductances and torque average value and ripple.

This work was supported by the Romanian Executive Agency for Higher Education, Research, Development and Innovation Funding (UEFISCDI) under the AUTOMOTIVE LOW-NOISE ELECTRICAL MACHINES AND DRIVES OPTIMAL DESIGN AND DEVELOPMENT (ALNEMAD) Joint Applied Research Project (PCCA) in the frame of "Partnerships" projects (PN II – National Plan for Research, Development and Innovation) and ADvanced Electric Powertrain Technology (ADEPT) project which is an EU funded Marie Curie ITN project, grant number 607361.

978-1-4799-7993-6/15/$31.00 ©2015 IEEE

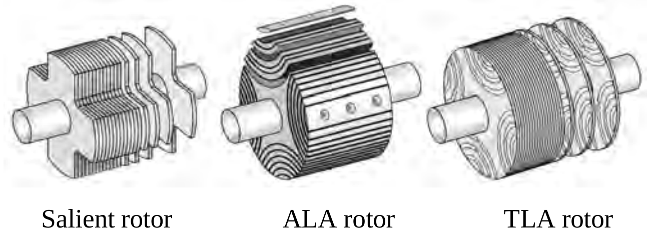

Fig. 1. Synchronous Reluctance Motor rotor types [9]

II. Design of the Synchronous Reluctance Machine

In the absence of permanent magnets or rotor winding, like in the widely used PMSM or Induction Machines, the SynRM operation relies on the reluctance torque, which depends on the saliency, defined as the ratio between the inductance in the direct and quadrature axes. Reluctance torque produced by the synchronous reluctance machine is equal to that of conventional synchronous machine with no field current and is given by the formula [10]:

$$T = p\frac{U_{phs}^2}{\omega_s}\left(\frac{1-\frac{X_q}{X_d}}{X_q}\right)\sin(2\delta) \qquad (1)$$

where: U_{phs} - stator phase voltage, p – pole pair number, ω_s – angular speed of rotating field, δ – current angle, X_d – reactance in direct axis, X_q – reactance in quadrature axis. The main goal when designing this type of machine is to maximize the saliency ratio so that the machine produces the maximum torque.

The current market of EV consists of a wide range of vehicle types, from small passenger cars with power ratings of 30 kW or less, like Smart Fortwo electric, up to high-end electric sports cars, with power rating of near 400 kW, like the AMG SLS E-Cell or Tesla Roadster. The electric power requirements depend on various parameters: maximum desired speed of the EV (off-highway or highway vehicle), acceleration performance, weight of the vehicle, maximum slope, etc.; all these influence the maximum speed and the maximum power of the electrical machine, while the desired range dictates the size of the battery pack and the efficiency of the electric drive. Starting from the requirements at vehicle level for a mid-range (H)EV a maximum electric power of 66 kW is considered as sufficient in this paper. Fig. 2 shows the torque/speed profile of the SynRM: a constant torque region, up to 4000 rpm, is considered, while constant power regime is used up to 12000 rpm; the four operating points that were considered in the simulations presented in this paper are highlighted in the figure, for peak (66 kW) and continuous power (22 kW) at 4000 and 12000 rpm.

The machine's length and diameter were obtained from the sizing equation given below [11]:

$$T = \sigma_{Ftan}\pi\frac{D_r^2}{2}l' \qquad (2)$$

where: σ_{Ftan} – tangential stress, D_r – diameter of the rotor, l' - effective length of the rotor.

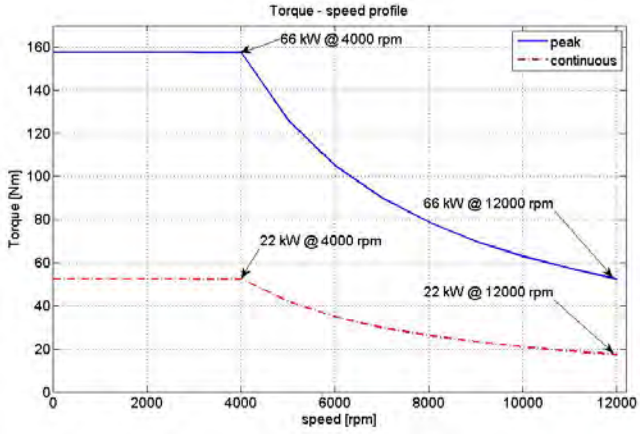

Fig. 2. Torque/speed profile for peak and continuous power

The basic dimensions of the machine are presented in table below.

TABLE I. Main Geometrical Dimensions

Parameter	Value
Rotor's radius	85.5 [mm]
Air gap length	0.5 [mm]
Stator's outer radius	130 [mm]
Shaft radius	22 [mm]
Number of flux barriers per pole	4
Number of poles	4

III. Synchronous Reluctance Machine Topologies

A large number of design parameters in the stator and rotor of the SynRM influence the performances of the machine, like the tooth width, yoke height, slot opening, number and positioning of the rotor flux barriers, etc. The present paper shows the influence of the number of stator slots and rotor barriers shapes on the torque average value and ripple.

A. SynRM Stator Topologies

One of the major advantages of the SynRM is the fact that stator structure is identical to the one used in conventional 3-phase Induction or Synchronous Machines, so the manufacturing process is more mature than in the case of other electrical machines. As a side effect, the SynRM is compatible with the control strategies and power electronics topologies used for IM or SM, so the overall cost of the drive system is lower compared to other electric machines used in EV applications.

Usually the number of slots of an electrical machine's stator is chosen based on the rated power and the main geometrical dimensions; in the case of the SynRMs presented in this paper the behavior of the machines is studied for 3 topologies: 24, 30 and 36 slots. For each case the outer and inner diameter of the laminations and the air gap are kept constant, along with the slot opening, width and depth. The 3 resulting structures are presented in Fig. 3.

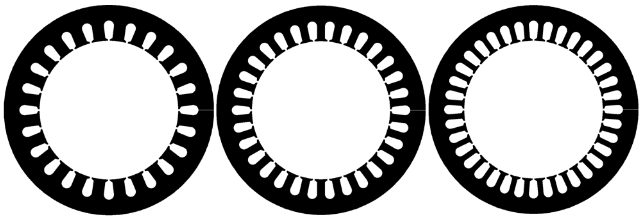

Fig. 3. SynRM stator structures

Different winding topologies were considered for each case and the most appropriate was used in the comparative study: full-pitch winding for the 24 slot structure, fractional pitch for the 30 slots structure and short-pitch winding for the 36 slots stator. Because the number of slots/pole/phase varies, different number of turns per coil was considered, so that the total number of turns per phase is similar for the 3 stators. Fractional slot concentrated windings were studied for this type of machine [12], but this was not considered in this paper because of the reported increase of torque ripple.

B. *SynRM Rotor Topologies*

The saliency ratio of the machine is obtained by inserting flux barriers in the transversally laminated rotor. The number of flux barriers and their thickness decide how much magnetic flux can penetrate the rotor in *d* and *q* axes. Flux in *d* axis should be as high as possible while flux in *q* axis should be minimized. Typical flux barriers are shown in picture below [13, 14].

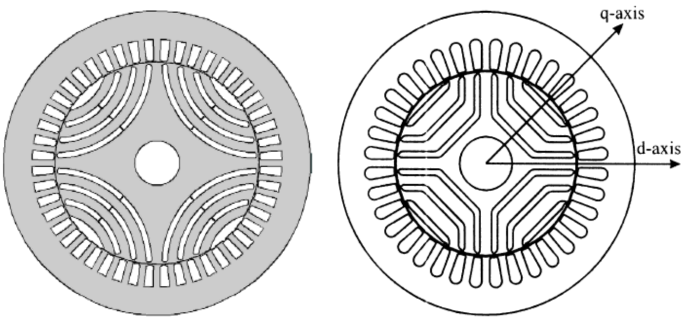

Fig. 4. Typical flux barrier shapes

To minimize the flux in *q* axis, the flux barriers should be as wide as possible, but at the same time the amount of iron in *d* axis is reduced which causes *d* axis flux to decrease. This is why it is so important to find the right thickness of flux barriers which give the maximized saliency ratio. The number of flux barriers is also very important. The optimal number of flux barriers is four; the improvement obtained by further increasing of the number of barriers would not be justified by the increase in terms of manufacturing problems and costs [14]. Shape of flux barriers is also significant since it decides about the permeance of flux path. Natural flux lines in solid rotor are presented in Fig.5.

Their shape can be described by Zhukovski function [13]. By solving the following equation for different values of parameters *a* and *v*, one can obtain the set of curves [15] which can be used to create flux barriers.

$$2xy - \frac{2xya^2}{x^2+y^2} = v \tag{3}$$

IV. RESULTS

In order to compare the performances of the different topologies electromagnetic simulations were performed in JMAG Designer, a FEM based commercial software. A series of static analysis were performed in order to determine the specific position were the rotor's *d*-axis is fully aligned with the stator magnetic field produced by the 3-phase winding.

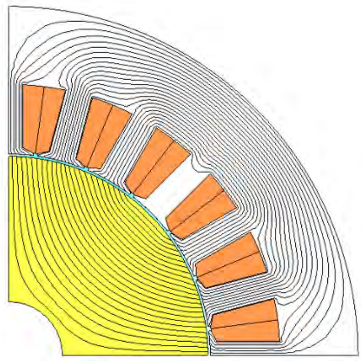

Fig. 5. Natural flux lines in machine with solid rotor

Fig. 6 shows the magnetic flux lines and the distribution of the magnetic flux density in modeled structures. The left column presents the conventional rotor SynRMs with round barriers, while the motor with "Zhukovski" shaped barriers are shown on the right. One can notice that the initial rotor position is different for the two barrier shapes because of the different methods used for creating the model: the "Zhukovski" barrier rotor has the *d*-axis drew on the symmetry of the model, while for the initial rotor there is a 45 degrees between the *d*-axis and the symmetry line.

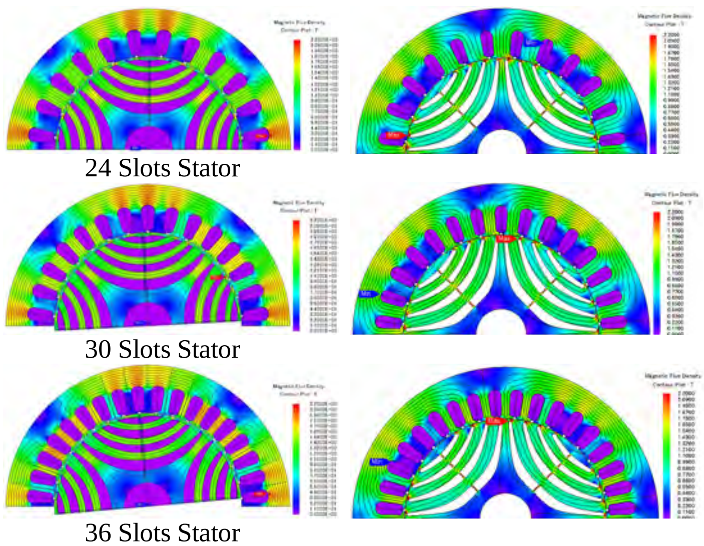

Fig. 6. Magnetic flux density and flux lines

The air gap magnetic flux density distributions obtained for these rotor positions in the 22kW @ 4000 rpm operating point are presented in Fig. 7; the radial component is plotted along the entire air gap circumferential length when stator magneto-motive force was applied in *d* axis. It was calculated to show how rotor topology affects magnetic flux distribution in the air gap in no load state. In the case of the 24 slots stator the air gap magnetic flux density of the "Zhukovski" shaped barrier rotor is closer to the ideal (sinusoidal) shape but the average value remains similar for both rotor types. For the 30 and 36 slots structures the asymmetries are caused by the different distance between the flux barriers, determining the stator teeth to align with the rotor flux paths in a different manner.

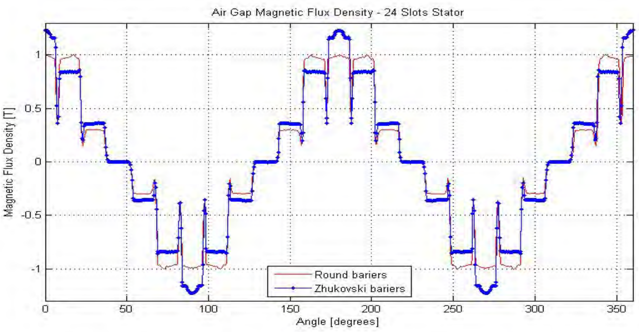

24 Slots Stator

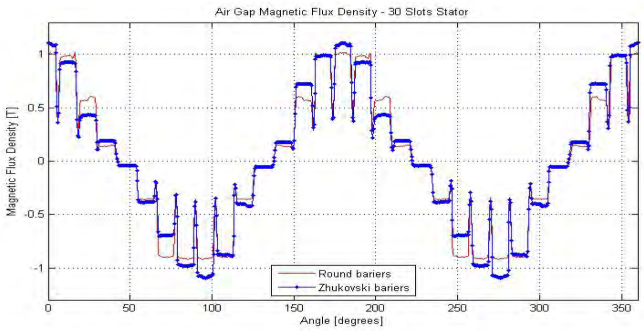

30 Slots Stator

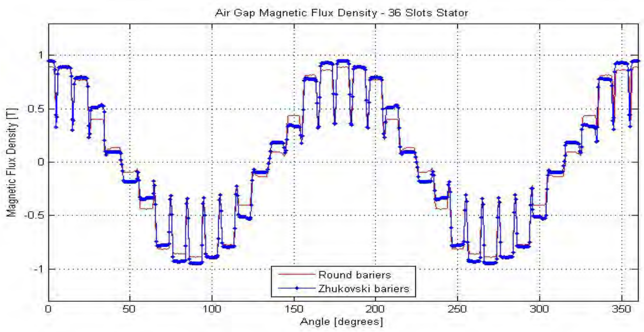

36 Slots Stator

Fig. 7. Air gap magnetic flux density repartition

The two pictures in Fig. 8 show the coil flux variation of machine with 36 slots and two rotor topologies. Only the first phase of each machine was supplied from DC current source while the rotor was rotating with constant revolution speed. Flux values of first phase coil were measured for rotor positions from 0 to 180 degrees with two degrees step. For machine with 36 slots in the stator, the flux was measured for current values from 5 A to 140 A with 5 A step. One can see that the flux waveform has two maximum and two minimum points. It is because the machine has four poles. Maximum value of the flux was achieved when *d* axis of the rotor was aligned with the axis of the coil. When rotor's *q* axis was aligned with the axis of the coil, the flux reached its minimum value. By dividing the maximum flux value by the corresponding current value, one can obtain inductance L_d in *d* axis whereas division of the minimum flux value by the current gives the *q*-axis inductance L_q. This test was performed to calculate the saliency ratio $\frac{L_d}{L_q}$ of the machine. One can notice that in case of Zhukovski type flux barriers, the coil flux is smaller than that of machine with round barriers.

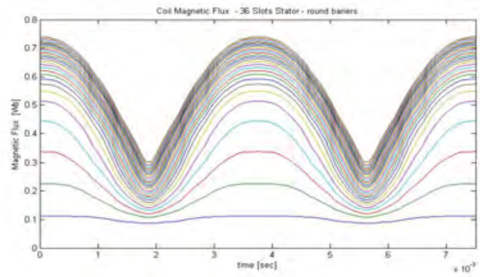

Round barriers

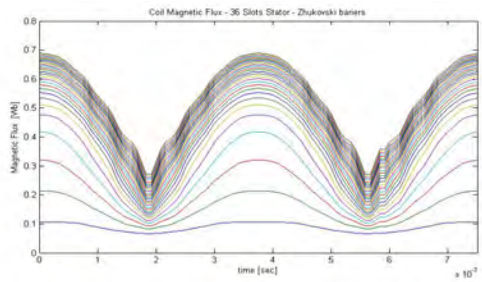

Zhukovski barriers

Fig. 8. Coil magnetic flux variation

Fig. 9 presents saliency ratios comparison for all machine topologies. One can see that in case of Zhukovski type flux barriers, the saliency ratio is higher for all three types of stator. It is also worth mentioning that despite the lower value of coil flux for Zhukovski type barriers in machine with 36 stator slots, the saliency ratio is still higher for machine with that type of rotor. The highest values of saliency ratios are achieved for machine with 30 stator slots and Zhukovski flux barriers.

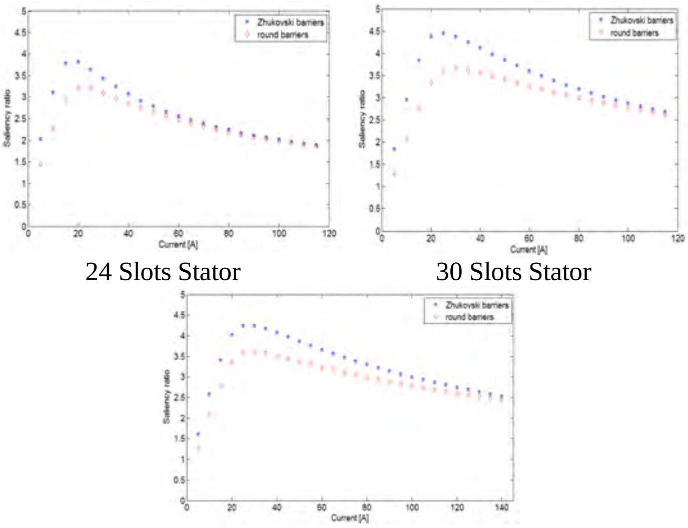

24 Slots Stator 30 Slots Stator

36 Slots Stator

Fig. 9. Saliency ratios as function of current

In Fig. 10 one can see instantaneous torque of all machine topologies. The waveform in the top of each figure is the torque at peak power whereas the bottom waveform shows the torque at continuous power.

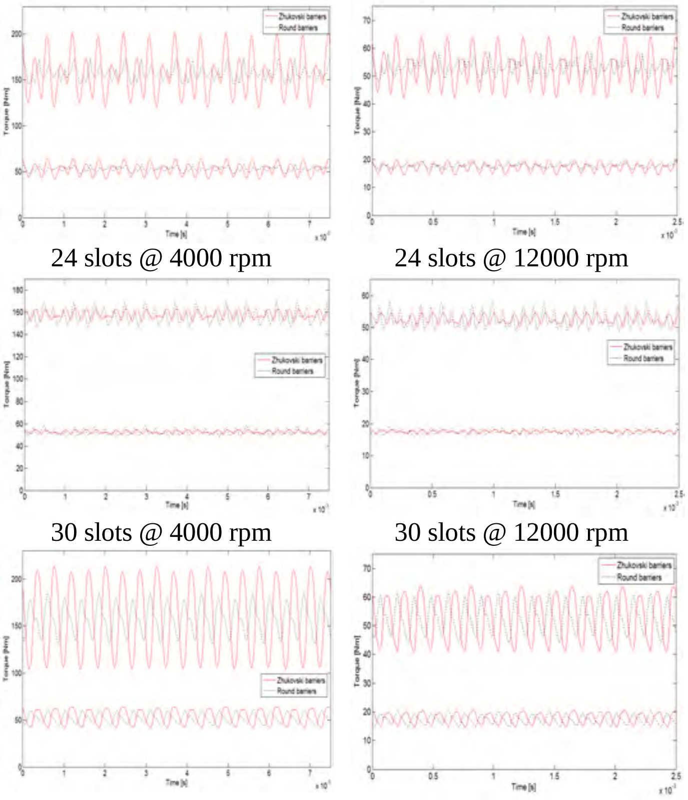

24 slots @ 4000 rpm 24 slots @ 12000 rpm

30 slots @ 4000 rpm 30 slots @ 12000 rpm

36 slots @ 4000 rpm 36 slots @ 12000 rpm

Fig. 10. Torque comparison of instantaneous torque of all machine topologies

Red continuous line shows the torque waveform of machine with Zhukovski's type flux barriers in the rotor and black dotted line shows torque waveform of machine with round barriers in the rotor. One can see relevant difference in torque ripple for each case between those two rotor types.

Based on the torque variation data the integral average and the ripple content were calculated and included in Table II. The table also contains information about the current required to reach the desired average torque for each of the 24 cases. As a general trend the current required for the topologies using the Zhukovski shaped barriers is smaller than the one used in the conventional structures to obtain the same average torque, meaning that the new structures exhibit higher efficiency. An exception is represented by the 36 slots structure, where the current values are lower when using round barriers; this is partially because although the saliency ratio is higher, the coil flux values are lower.

If the torque ripple is considered, one could notice that for the 24 and 36 slots SynRM the Zhukovski barrier structures exhibit higher ripple values; this problem could be partially solved by optimizing the radial repartition of the four barriers. The best results in terms of torque ripple and current decrease for the same average torque are obtained for the 30 slots structure with Zhukovski shaped flux barriers, where the ripple is halved compared to the initial geometry and the current required to obtain the same average torque is reduced by about 8%.

TABLE II. TORQUE VALUES

Case				Results		
Stator	***Speed [rpm]***	***Operating Point***	***Rotor***	***Peak Current [A]***	***Average Torque [Nm]***	***Torque ripple [%]***
24 slots	4000	Cont.	Round.	42.5	52.8	19.57
			Zhuk.	39	52.9	41.12
		Peak	Round.	113	157.08	17.67
			Zhuk.	106	157.17	51.56
	12000	Cont.	Round.	21.6	17.8	15.54
			Zhuk.	18	17.3	30.71
		Peak	Round.	42.5	52.8	19.57
			Zhuk.	39	53.1	41.41
30 slots	4000	Cont.	Round.	46.2	52.36	18.07
			Zhuk.	43	52.69	8.77
		Peak	Round.	123	156.69	14.85
			Zhuk.	118	157.77	7.75
	12000	Cont.	Round.	24	17.47	18.28
			Zhuk.	20	17.58	9.54
		Peak	Round.	46.2	52.39	18.01
			Zhuk.	43	52.68	8.78
36 slots	4000	Cont.	Round.	47.5	52.23	33.14
			Zhuk.	49	53.09	41.54
		Peak	Round.	130.1	157.32	34.13
			Zhuk.	134	158.66	68.66
	12000	Cont.	Round.	24.2	17.48	30.93
			Zhuk.	23	17.87	32.08
		Peak	Round.	47.7	52.51	33.14
			Zhuk.	48.5	52.47	43.15

V. CONCLUSIONS

The current paper focuses on a Synchronous Reluctance Motor with a peak power of 66kW and a maximum speed of 12000 rpm, which is considered appropriate for a mid-range EV. Three different stator topologies are considered, having 24, 30 and 36 slots, respectively and two rotor designs: the conventional round barriers and a new design that follows the natural flux lines in a solid rotor, described by the Zhukovski function.

The air gap magnetic flux density repartition is shown for all the structures, showing that when using the new barrier shape the variation is closer to the ideal sinusoidal form. Since the SynRM torque is depending on the ratio between the direct and quadrature inductances the variation of coil magnetic flux was studied, considering a constant current through one of the phases, so the maximum and the minimum inductances, corresponding to the *d* and *q* axes, respectively, could be determined. The results showed that the new rotor geometry has higher saliency at low currents, while for high currents the ratio is almost equal because of the saturation of the magnetic circuit.

The average value and ripple ratio of the torque was determined for the 4 characteristic operating points, showing that for the 24 and 30 slots structures a lower current is required when using the “Zhukovski” shaped barriers to get the same torque than in the case of the round shaped barriers; for the 36 slots structure the conventional rotor seems to be more efficient than the new variant. In the case of the 24 and 36 slots stators the torque ripple are higher when using the new barrier shapes, so further analysis on the location of the barriers must be performed. Promising results are obtained in the case of the 30 slots stator that exhibits lower torque ripple values compared to the other stator topologies. When using the “Zhukovski” shaped barriers the ripple is further reduced to half the value calculated for the conventional structure.

ACKNOWLEDGMENT

This work was supported by the Romanian Executive Agency for Higher Education, Research, Development and Innovation Funding (UEFISCDI) under the AUTOMOTIVE LOW-NOISE ELECTRICAL MACHINES AND DRIVES OPTIMAL DESIGN AND DEVELOPMENT (ALNEMAD) Joint Applied Research Project (PCCA) in the frame of "Partnerships" projects (PN II – National Plan for Research, Development and Innovation) and ADvanced Electric Powertrain Technology (ADEPT) project which is an EU funded Marie Curie ITN project, grant number 607361.

REFERENCES

[1] Zhu, Z.Q.; Howe, D., "Electrical Machines and Drives for Electric, Hybrid, and Fuel Cell Vehicles," Proceedings of the IEEE , vol.95, no.4, pp.746,765, April 2007

[2] Boldea, I.; Tutelea, L.N.; Parsa, L.; Dorrell, D., "Automotive Electric Propulsion Systems With Reduced or No Permanent Magnets: An Overview," Industrial Electronics, IEEE Transactions on , vol.61, no.10, pp.5696,5711, Oct. 2014

[3] J. Malan, M.J. Kamper: “Performance of a Hybrid Electric Vehicle Using Reluctance Synchronous Machine Technology”, IEEE Trans. on Industry Applications, vol. 37, no. 5, 2001

[4] W., Hanguang, L., Qiuhua, Y., Linjuan, "An investigation of the synchronous reluctance motors", Proc.of lCEMs' 2001 , China

[5] Boglietti, A.; Cavagnino, A.; Pastorelli, M.; Vagati, A., "Experimental comparison of induction and synchronous reluctance motors performance," Industry Applications Conference, 2005. Fourtieth IAS Annual Meeting. Conference Record of the 2005 , vol.1, no., pp.474,479 Vol. 1, 2-6 Oct. 2005

[6] Boglietti, A.; Pastorelli, M., "Induction and synchronous reluctance motors comparison," Industrial Electronics, 2008. IECON 2008. 34th Annual Conference of IEEE , vol., no., pp.2041,2044, 10-13 Nov. 2008

[7] Hsu, J.S.; Liou, S.-S.P.; Woodson, Herbert H., "Comparison of the nature of torque production in reluctance and induction motors," Energy Conversion, IEEE Transactions on , vol.5, no.2, pp.304,309, Jun 1990

[8] Kostko, J.K., "Polyphase reaction synchronous motors," American Institute of Electrical Engineers, Journal of the , vol.42, no.11, pp.1162,1168, Nov. 1923

[9] Jere Kohelmainen: "Synchronous Reluctance Motor With Form Blocked Rotor", IEEE Transactions on Energy Conversion, Vol. 25, No. 2, June, 2010.

[10] J. H. Lee, J. C. Kim, D. S. Hyun, „Hysteresis modeling of synchronous reluctance motor considering PWM input voltage”, Elsevier, Physica B 275, 2000

[11] Juha Pyrhonen, Tapani Jokinen, Valeria Hrabovcova, “Design of Rotating Electrical Machines”, John Wiley & Sons, 2008

[12] Spargo, C.M.; Mecrow, B.C.; Widmer, J.D., "Application of fractional slot concentrated windings to synchronous reluctance machines," Electric Machines & Drives Conference (IEMDC), 2013 IEEE International , vol., no., pp.618,625, 12-15 May 2013

[13] Jorma Haataja, “A Comparative Performance Study of Four-Pole Induction Motors and Synchronous Reluctance Motots in Variable Speed Drives”, Lappeenranta University of Technology, Doctoral Thesis, Lappeenranta, Finland, 2003

[14] Reza - Rajabi Moghaddam, “Synchronous reluctance machine (SynRM) in variable speed drives (VSD) applications”, Doctoral Thesis, Stockholm, Sweden, 2011

[15] Adam Marlewski, “Graphing Zhukovski transformation in Derive”, Proceedings 19th European Conference on Modelling and Simulation Yuri Merkuryev, Richard Zobel, Eugène Kerckhoffs © ECMS, 2005